CHAPTER 5

FIRST-PRINCIPLES INVESTIGRATION ON THERMOELECTRIC PROPERTIES OF $TiNiSn_{1-x}A_x$ (A = As, Sb, Bi; x = 0 – 0.125) HALF-HEUSLER ALLOYS

Introduction

So far, TiNiSn-based half Heusler thermoelectric materials provided the maximum dimensionless figure of merit (ZT) with value 1.5 at 700 – 800 K (Sakurada & Shutoh, 2005, p. 082105). To enhance the ZT, it should be considered the Seebeck coefficient (S), electrical conductivity (σ), and thermal conductivity (κ) as $ZT = S^2\sigma T/\kappa$, where T is absolute temperature. Besides, high ZT should high power factor ($S^2\sigma$) and low κ (Aswal, Basu & Singh, 2016, pp. 50-67). Previous works we have theoretical investigated the thermoelectric (TE) properties of an element doping on the Ti-site TiNiSn. We found that the transition metals (TM) can be reduced the lattice thermal conductivity by 27% (Rittiruam, Yangthaisong & Seetawan, 2018). The TM co-doped on the Ti-site gives an electron to TiNiSn and appears in electron pocket (Rittiruam, Yangthaisong & Seetawan, 2018, p. 175101). Therefore, the elements doping on Ti-site become clear. So far, the Sb doping on Sn-site reduces the electrical resistivity and enhances the power factor at 300 K. Then, Lei et al. (2017, pp. 9343-9347). revealed the TE properties of $TiNiSn_{1-x}Sb_x$ at middle temperature-range. They reported that the Sb significantly enhanced ZT at low doping-concentration, which is our motivation for study in electronic structure. In

addition, Sb is a group 5A element. The isolate element of Sb composed As and Bi in predict table for Heusler alloys. In this work, we investigated the electronic structure and TE properties of $TiNiSn_{1-x}A_x$, where A is As, Sb and Bi, and x = 0 – 0,125. All of investigation performed under the first–principles density functional theory–based.

Computational details

The As, Sb, and Bi doping on Sn–site as $TiNiSn_{1-x}A_x$ (where A is As, Sb, and Bi; x = 0 – 0.125) crystal structure was designed using the MgAgAs–type structure (Vilars & Calvert, 1991) with space group number 216. We employed the CIF2Cell package (Björkman, 2011) to make a 2×2×2 supercell. The supercell composed of a total of 96 atoms showed $Ti_{32}Ni_{32}Sn_{32-x}A_x$ for $TiNiSn_{1-x}A_x$. The electronic structure was investigated by density functional theory (DFT) (Hohenberg & Kohn, 1964; Kohn & Sham, 1965) with the projector augmented wave (PAW) within the Vienna ab initio simulation package (VASP) (Kresse & Hafner, 1993, p.558; 1994, p. 14251; Kresse, 1996, p.15; Kresse & Furthmüller, 1996, p.11169). The exchange–correlation function used the generalized gradient approximation (GGA) (Rappe, Rabe, Kaxiras & Joannopoulos, 1990) and Perdew, Burke and Ernzerhof (PBE) functional (Perdew, Burke & Ernzerhof, 1996). The 4×4×4 Monkhorst–Pack *k*–mesh Brillouin zone (BZ) integration, kinetic energy cut–off of 540 eV, and convergence threshold of 1×10^{-6} were used for self–consistent field calculation. The transport properties were investigated by Boltzmann transport theory with the constant scattering time approximation (CSTA) and Fourier interpolation of the calculated bands based on BoltzTraP code (Madsen & Singh, 2006). The transport properties were calculated with:

$$\sigma = \frac{1}{\Omega}\int \Xi(\varepsilon)\left[-\frac{\partial f_0}{\partial \varepsilon}\right] d\varepsilon, \tag{81}$$

$$S = \frac{1}{eT\Omega\sigma} \int \Xi(\varepsilon)(\varepsilon - \mu) \left[-\frac{\partial f_0}{\partial \varepsilon} \right] d\varepsilon, \quad (82)$$

$$\Xi(\varepsilon) = \sum \vec{v}_\alpha \vec{v}_\beta \, \tau, \quad (83)$$

where Ω is reciprocal space volume, f_0 is the Fermi–Dirac distribution function, ε is an eigen energy of each band structure, e is the electron charge, Ξ is the transport distribution, τ is the scattering time, $\vec{v}$ is the group velocity, and α and β are mean tensors. The total thermal conductivity (κ_{tot}) includes the electron (κ_{e}) and lattice (κ_{lat}) thermal conductivity. The value of κ_{e} was calculated by using the Wiedemann–Franz law as in the equations:

$$\kappa_{\mathrm{e}} = \sigma L T, \quad (84)$$

$$L = 1.5 + \exp[-\frac{|S|}{116}], \quad (85)$$

where L is the Lorenz number, and S is in μVK^{-1} (Kim, Gibbs, Tang, Wang & Snyder, 2015). The κ_{lat} was calculated using second–order (harmonic) interatomic force constants (IFCs) as implemented the phono3py package (Togo, Oba & Tanaka, 2008, p.134106; Togo, Chaput & Tanaka, 2015, p.094306). From the phono3py package, the heat capacity (C_λ) in the physical unit eV/K defined by

$$C_\lambda = k_{\mathrm{B}} \left(\frac{\hbar\omega_\lambda}{k_{\mathrm{B}}T} \right)^2 \exp(\hbar\omega_\lambda / k_{\mathrm{B}}T) \left[\exp\left(\frac{\hbar\omega_\lambda}{k_{\mathrm{B}}T} \right) - 1 \right]^{-2}. \quad (86)$$

The thermal conductivity tensors at k–star ($^*\mathbf{k}$) as $\sum_{\mathbf{q}\in{}^*\mathbf{k}} \kappa_{\mathbf{q}j}$. The of this over $^*\mathbf{k}$ corresponding to irreducible q–points divided by number of grid point gives κ. Each tensor element is the sum of tensor elements on the members of $^*\mathbf{k}$ for example, symmetrically equivalent q–points by crystallographic point group and time reversal symmetry. Outer products of group velocities ($\mathbf{v}_\lambda$) for k–stars ($^*\mathbf{k}$) for each irreducible q–point and phonon band (j) as $\sum_{\mathbf{q}\in{}^*\mathbf{k}} \mathbf{v}_{\mathbf{q}j} \otimes \mathbf{v}_{\mathbf{q}j}$. Averaged phonon–phonon interaction ($P_{\mathbf{q}j}$) in eV^2 is

$$P_{\mathbf{q}j} = \frac{1}{(3n_{\mathrm{a}})^2} \sum_{\lambda'\lambda''} |\Phi_{\lambda\lambda'\lambda''}|^2. \quad (87)$$

The κ_{lat} calculated using C_λ, and $\mathbf{v}_\lambda$ with the single mode relaxation time (SMART) method, a mode contribution to the κ_{lat} is given by

$$\kappa_{\mathrm{lat}} = \frac{1}{V} C_\lambda \mathbf{v}_{\mathrm{q}j} \otimes \mathbf{v}_{\mathrm{q}j} \tau_\lambda^{\mathrm{SMART}} , \tag{88}$$

where, V is the volume of crystal structure.

To understand the stability of elements doping Sn–site, we calculated the enthalpy formation energy (ΔH_f) and defect formation energy (E_f) according to equations. (79) and (80) (Rittiruam et al., 2018, p. 175101):

$$\Delta H_f(\mathrm{TiNiSn_{1-x}A_x}) = E(\mathrm{TiNiSn}) - E^{\mathrm{bulk}}(\mathrm{Ti}) - E^{\mathrm{bulk}}(\mathrm{Ni}) - (1-x)E^{\mathrm{bulk}}(\mathrm{Sn}) - (x)E^{\mathrm{bulk}}(\mathrm{A}), \tag{89}$$

$$E_f(\mathrm{TiNiSn_{1-x}A_x}) = E(\mathrm{TiNiSn_{1-x}A_x}) - E(\mathrm{TiNiSn}) - E(\mathrm{A}) + E(\mathrm{Sn}), \tag{90}$$

where $E(\mathrm{TiNiSn})$ and $E(\mathrm{TiNiSn_{1-x}A_x})$ are the total energy of TiNiSn and $TiNiSn_{1-x}A_x$ obtained from the supercell. $E^{\mathrm{bulk}}(\mathrm{Ti})$, $E^{\mathrm{bulk}}(\mathrm{Ni})$, $E^{\mathrm{bulk}}(\mathrm{Sn})$, and $E^{\mathrm{bulk}}(\mathrm{A})$ are the total energies in their bulk phases of Ti, Ni, Sn, and the group 5A elements, respectively.

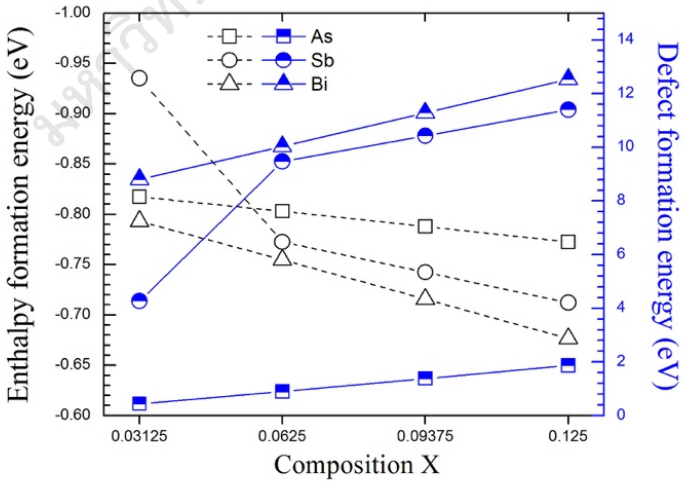

Figure 33 The enthalpy formation energy and defect formation energy for $TiNiSn_{1-x}A_x$.

Results and Discussion

The ΔH_f and E_f of $TiNiSn_{1-x}A_x$ illustrated in Figure 33. The ΔH_f shows negative value and means these alloys are exothermic reaction and can synthesis. Besides, the E_f decreases with increasing by composition *x*. These behaviors imply that the $TiNiSn_{1-x}A_x$ (A = As, Sb, and Bi; x = 0 – 0.125) become more stable at the low composition *x*.

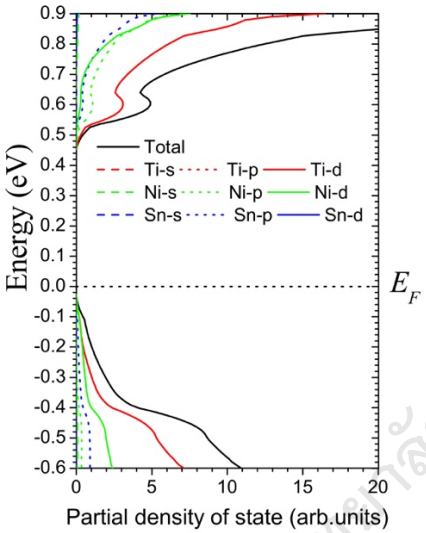

Figure 34 The partial density of state for TiNiSn.

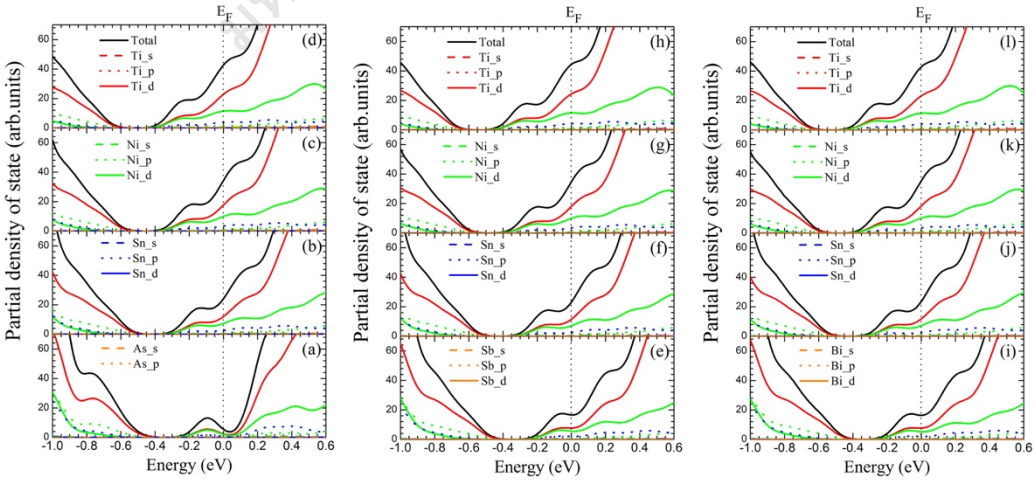

Figure 35 The partial density of state for $TiNiSn_{1-x}A_x$ (A = As, Sb, and Bi; x = 0 – 0.125).

In order to understand the As, Sb, and Bi–doping on the Sn site TiNiSn, we calculated the electronic structure likely density of state (DOS) and band structure. Figure 34 shows the DOS of TiNiSn. The negative and positive value of an energy is electron–filled (valence band, VB) and empty state (conduction band, VB). The Fermi level (E_F) sets in zero energy. The DOS of TiNiSn provides the energy gap value of 0.46 eV and agrees with previous work (Rittiruam et al., 2018, p. 175101). Figure 35 illustrates the DOS of $TiNiSn_{1-x}A_x$ (A=As, Sb, Bi). It is shows that the CB shifted down into the E_F in doping case. The valence electron is four for Sn and five for As, Sb and Bi. The As–, Sb– and Bi–doped in Sn–site shows electron–filled state in CB. The area of the CB in E_F can be called that electron pocket. The electron pocket increased with increasing by the doping–concentration. In addition, the Ti–d and Ni–d state play important rule in both CB and VB for TiNiSn in Figure 34. The DOS of doping case shows Ti–d and Ni–d increased at E_F. It should be that As, Sb and Bi give an electron to Ti– and Ni–site rather than Sn–site. Figure 36 shows the band structure of doping case. The electron pocket can observe in the Γ point.

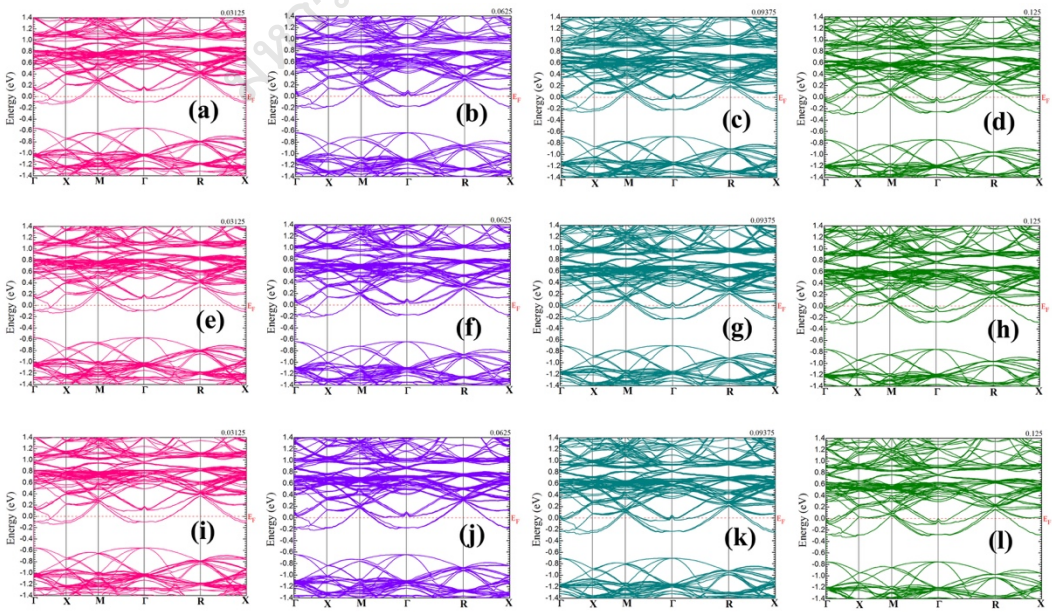

Figure 36 The band structure for $TiNiSn_{1-x}A_x$ (A = As, Sb, and Bi; x = 0 – 0.125).

The thermoelectric properties included electrical and thermal part. The electrical part illustrated in Figures 37–39. Figure 37 shows the Seebeck coefficient together with references (Katayama, Kim, Kimura & Mishima, 2003, pp. 1160–1165; Lei et al., 2017, pp. 9343–9347) versus temperature. The Seebeck coefficient of TiNiSn is about –300 μVK^{-1} at 300 K (Katayama et al., 2003, pp. 1160–1165). In previous work (Rittiruam, Yangthaisong & Seetawan, 2018, pp. 7456–7462), we have the Seebeck coefficient about –320 μVK^{-1} at 300 K and then it decreases to –150 μVK^{-1} at 1000 K. The As doping case shows the Seebeck coefficient with value –265 μVK^{-1} for x = 0.03125 decreased to –28 μVK^{-1} for x = 0.125 at 300 K, respectively. The small Seebeck coefficient means this material become metallic. By the way, Figure 37(A) shows Seebeck coefficient of x = 0.03125 decreased with increasing by temperature. This is semiconductor behavior. The Seebeck coefficient of A = Bi less than Sb and As at same composition x. The Seebeck coefficient of A = As, Sb, Bi with composition x = 0.0625 – 0.125 decreased with the temperature increasing, which is a metallic behavior. We confirmed above mentioned by the electrical conductivity (Aswal et al., 2016, pp. 50–67). We used the electrical conductivity from the experimental data of Reference (Lei et al., 2017, pp. 9343–9347) to calculate the electrical conductivity, this method revealed in References (Sun & Singh, 2016, p.104803). Figure 38 shows the electrical conductivity increased with doping by As, Sb and Bi. As well know the Seebeck coefficient and electrical conductivity yielded the power factor (PF) as $PF = S^2\sigma$. The PF versus temperature illustrated in Figure 39. The high PF appeared in low doping–concentration (< 0.0625).

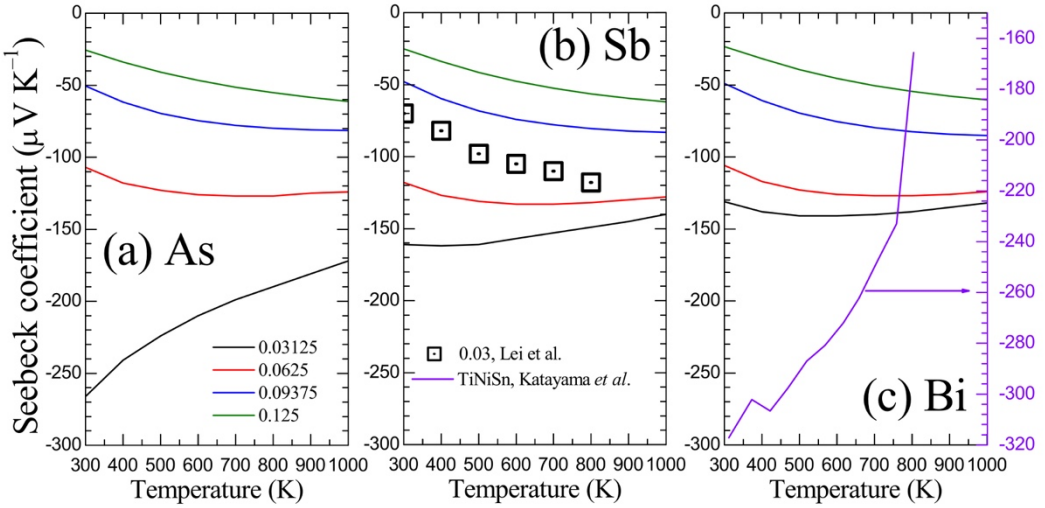

Figure 37 The Seebeck coefficient versus temperature for $TiNiSn_{1-x}A_x$

(A = As, Sb, and Bi; x = 0 – 0.125).

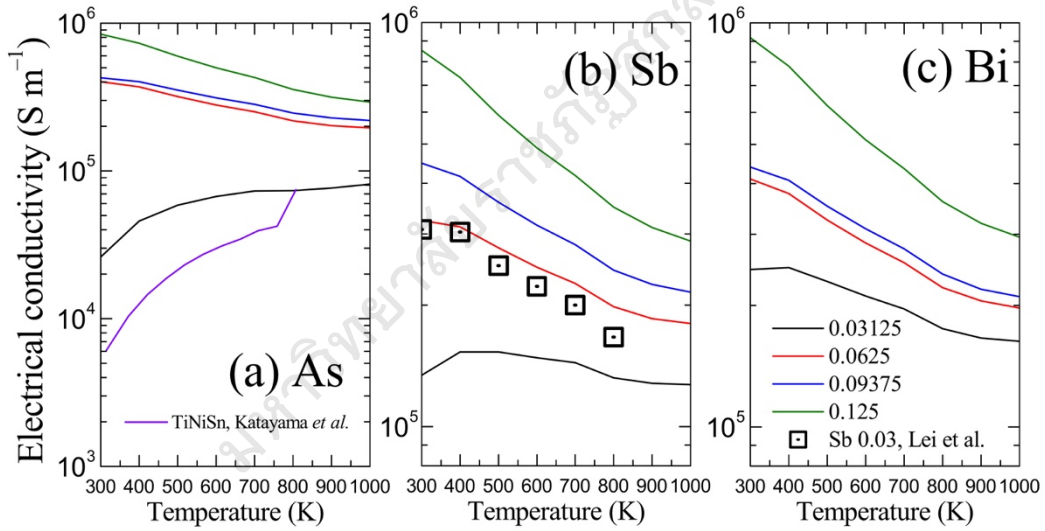

Figure 38 The electrical conductivity versus temperature for $TiNiSn_{1-x}A_x$

(A = As, Sb, and Bi; x = 0 – 0.125).

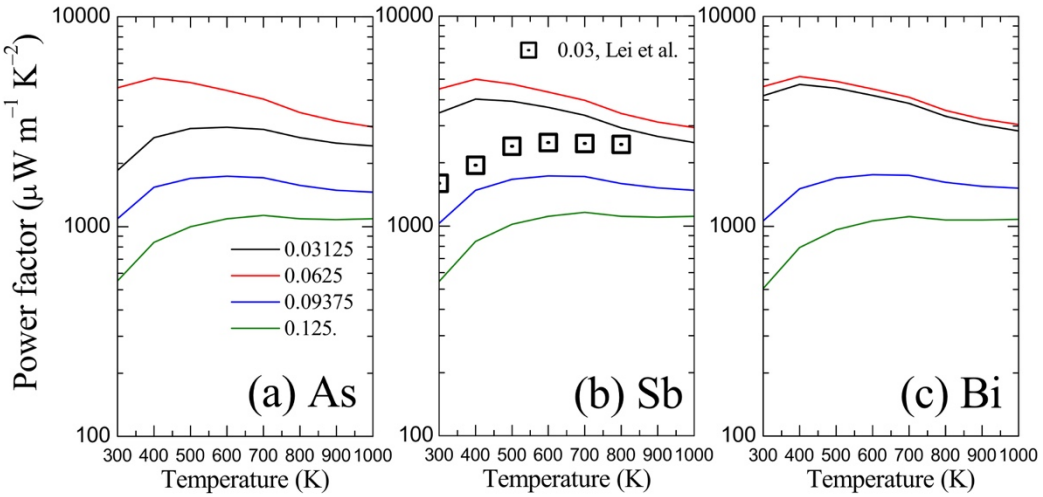

Figure 39 The power factor versus temperature for $TiNiSn_{1-x}A_x$ (A = As, Sb, and Bi; x = 0 – 0.125).

In thermal part, we considered in thermal conductivity. Figure 40 shows the κ_e versus temperature. It was found that the κ_e increased with increasing temperature due to the electrical conductivity. Besides, the κ_e of A = Bi are more than As and Sb. The κ_e value of these alloys more than an oxide materials (Sun & Singh, 2016, p.104803). Figure 41 plays the κ_{lat} versus temperature. The calculated κ_{lat} value of TiNiSn is 6.3 $Wm^{-1}K^{-1}$ at 300 K decreased to 1.9 $Wm^{-1}K^{-1}$ at 1000 K in good agreement with reference (Ding, Gao & Yao, 2015, p.235302). We found that the As, Sb and Bi reduced the κ_{lat} from 6.2 $Wm^{-1}K^{-1}$ to 3.4 $Wm^{-1}K^{-1}$ at 300 K. The minimum κ_{lat} is 4.1 $Wm^{-1}K^{-1}$ for $TiNiSn_{0.875}As_{0.125}$, 3.7 $Wm^{-1}K^{-1}$ for $TiNiSn_{0.9375}Sb_{0.0625}$, and 3.4 $Wm^{-1}K^{-1}$ for $TiNiSn_{0.875}Bi_{0.125}$, at 300 K, respectively.

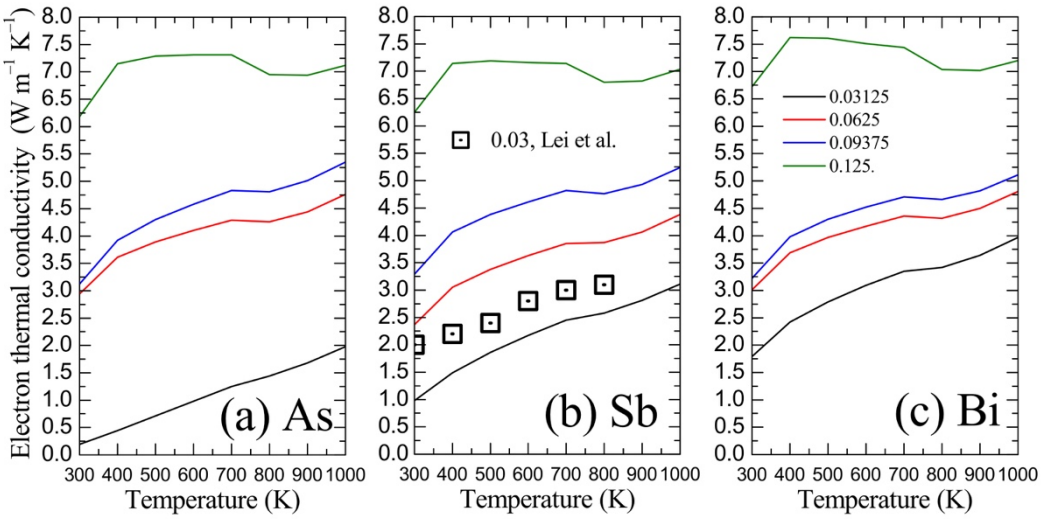

Figure 40 The electron thermal conductivity versus temperature for $TiNiSn_{1-x}A_x$ (A = As, Sb, and Bi; x = 0 – 0.125).

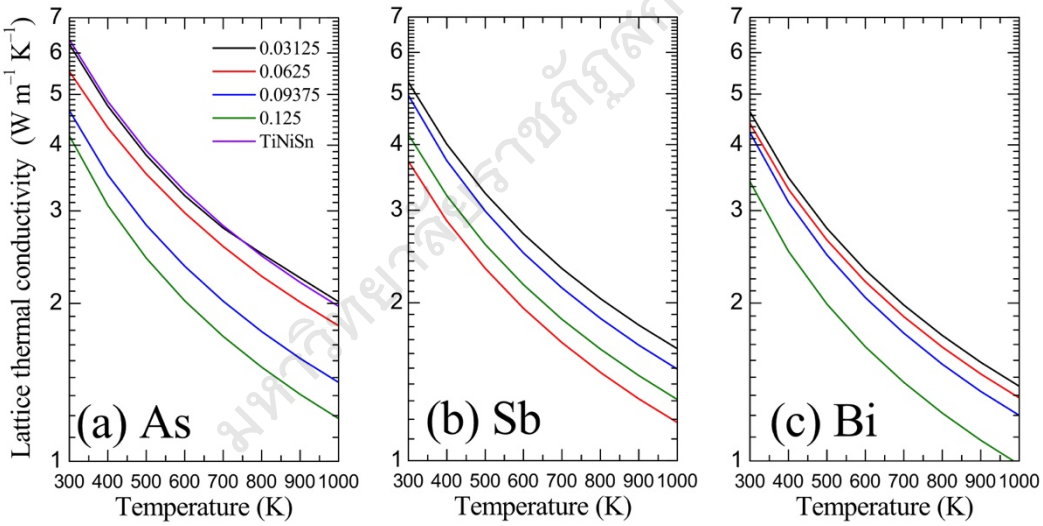

Figure 41 The lattice thermal conductivity versus temperature for $TiNiSn_{1-x}A_x$ (A = As, Sb, and Bi; x = 0 – 0.125).

To explain the As, Sb and Bi induced the $\kappa_{\mathbf{lat}}$ of TiNiSn, we calculated the phonon dispersion and phonon density of state (phDOS) as shown in Figures 42–46. The phonon dispersion of TiNiSn (Figure 42) shows the frequency from 0 to ~150 cm^{-1} and separated from ~150 to ~200 cm^{-1}. The frequency from 0 to ~150 cm^{-1} is acoustic mode and frequency from ~150 to ~200 cm^{-1} is optical mode. The group

velocity ($\mathbf{v_g}$) can calculated by $\mathbf{v_g} = \partial\omega/\partial\mathbf{k}$, where ω is frequency. The calculated $\mathbf{v_g}$ of TiNiSn is 3824 (Ding et al., 2015, p.235302). The phonon dispersion of TiNiAs, TiNiSb and TiNiBi illustrated in Figures 43–45. We found that the optical mode closed to the acoustic mode in TiNiAs. For TiNiSb and TiNiBi, the phonon dispersion shows the slop in acoustic mode less than TiNiSn, and it means the Sb and Bi can reduce $\mathbf{v_g}$ of TiNiSn. Figure 46 shows the phDOS of TiNiSn, TiNiAs, TiNiSb, and TiNiBi. It is clearly that the acoustic mode of TiNiAs, TiNiSb and TiNiBi appeared in low frequency.

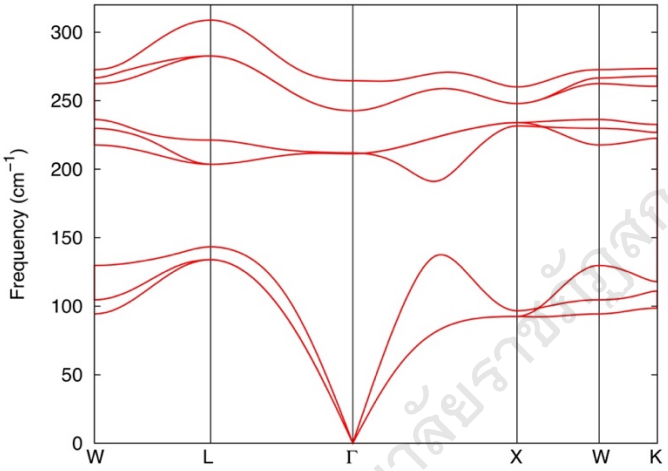

Figure 42 The phonon dispersion for TiNiSn.

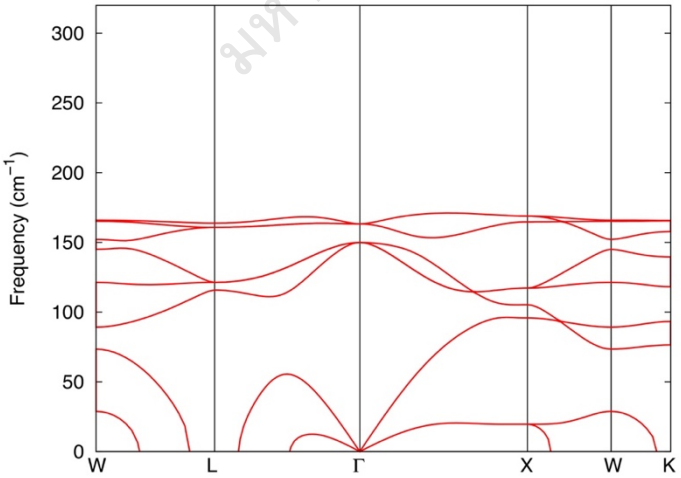

Figure 43 The phonon dispersion for TiNiAs.

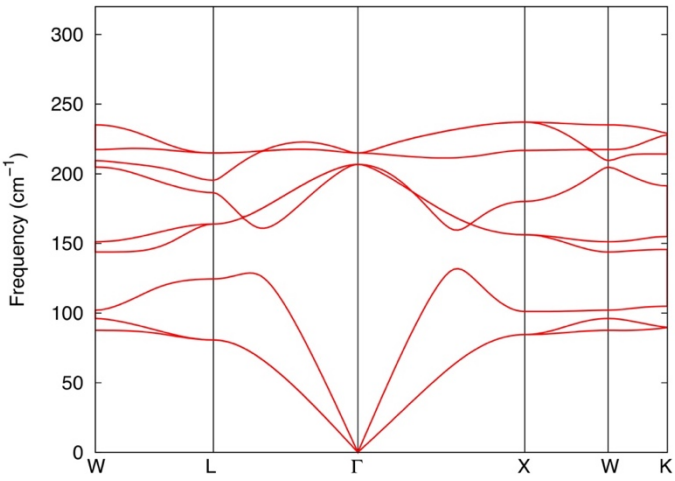

Figure 44 The phonon dispersion for TiNiSb.

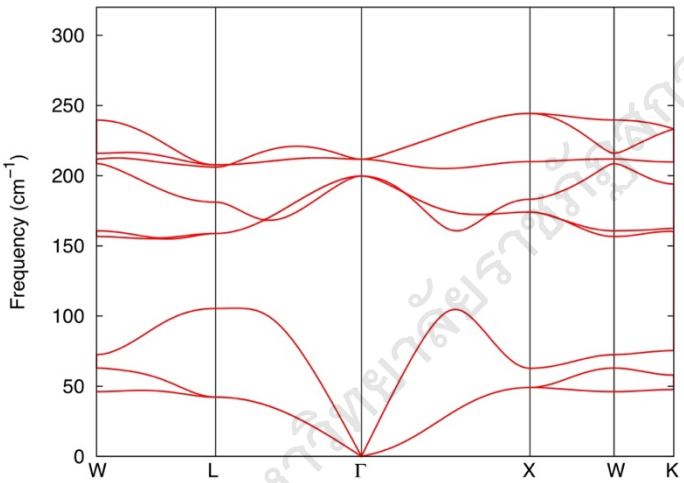

Figure 45 The phonon dispersion for TiNiBi.

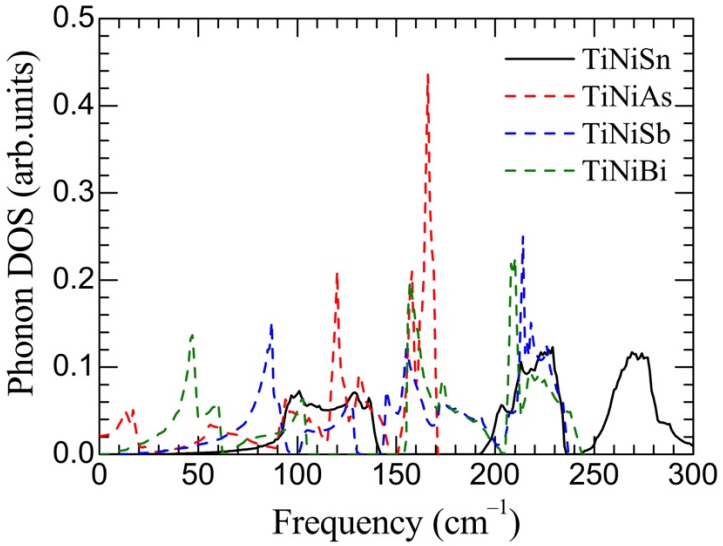

Figure 46 The phonon density of state for TiNiSn, TiNiAs, TiNiSb, and TiNiBi.

Figure 47 shows the $\kappa_{\mathbf{tot}}$ versus temperature for $TiNiSn_{1-x}A_x$. The minimum value of $\kappa_{\mathbf{tot}}$ appeared in As x = 0.03125, Sb x = 0.03125 and 0.0625, and Bi x = 0.03125, respectively. Although the elements group 5A enhanced the electrical part the $\kappa_{\mathbf{tot}}$ not directly enhanced. The As with x = 0.03125 significantly decreased the $\kappa_{\mathbf{tot}}$ of TiNiSn rather than Sb and Bi. In addition, the maximum ZT obtained by As with x = 0.03125 with value of 0.6 at 1000 K. The calculated ZT of Sb with x = 0.03125 agrees with the experimental data of reference (REF). The element group 5A with small doping concentration can be increased the ZT of TiNiSn up to 0.5 at 1000 K.

To confirm As, Sb, and Bi give an electron and enhance the carrier concentration to TiNiSn, we calculated the Hall carrier concentration as equation

$$n_{\mathrm{H}} = \frac{1}{eR_{\mathrm{H}}}, \tag{91}$$

where e is an electron charge. n_{H} and R_{H} are Hall carrier concentration and Hall coefficient. We found that element group 5A increased the Hall carrier concentration from 2×10^{17} cm^{-3} (TiNiSn) up to ~3×10^{21} cm^{-3}, as shown in Figure 49.

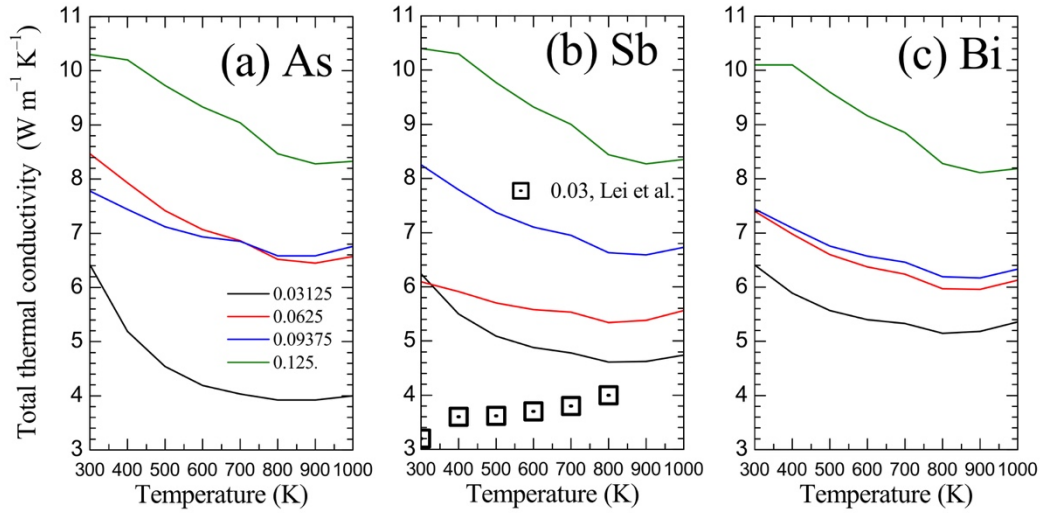

Figure 47 The total thermal conductivity versus temperature for $TiNiSn_{1-x}A_x$ (A = As, Sb, and Bi; x = 0 – 0.125).

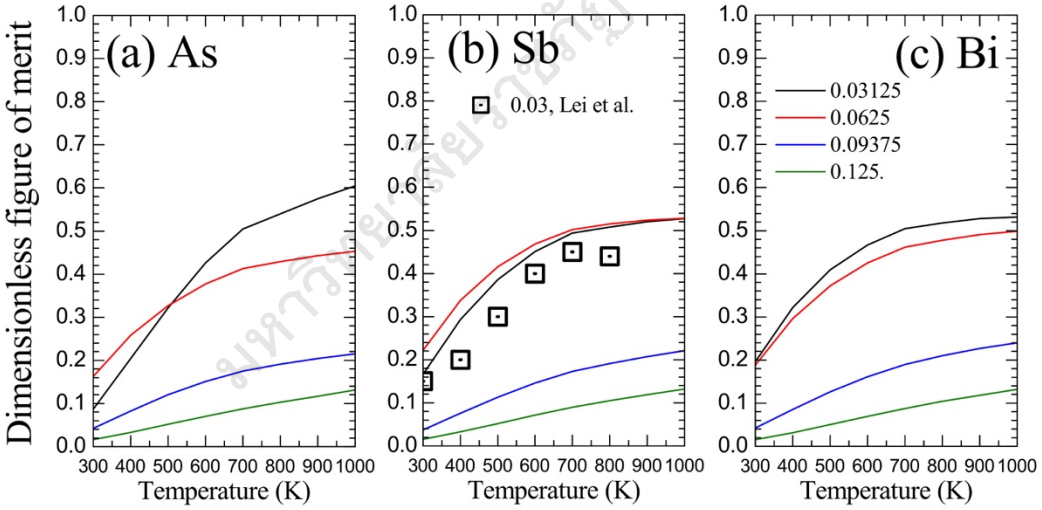

Figure 48 The dimensionless figure of merit versus temperature for $TiNiSn_{1-x}A_x$ (A = As, Sb, and Bi; x = 0 – 0.125).

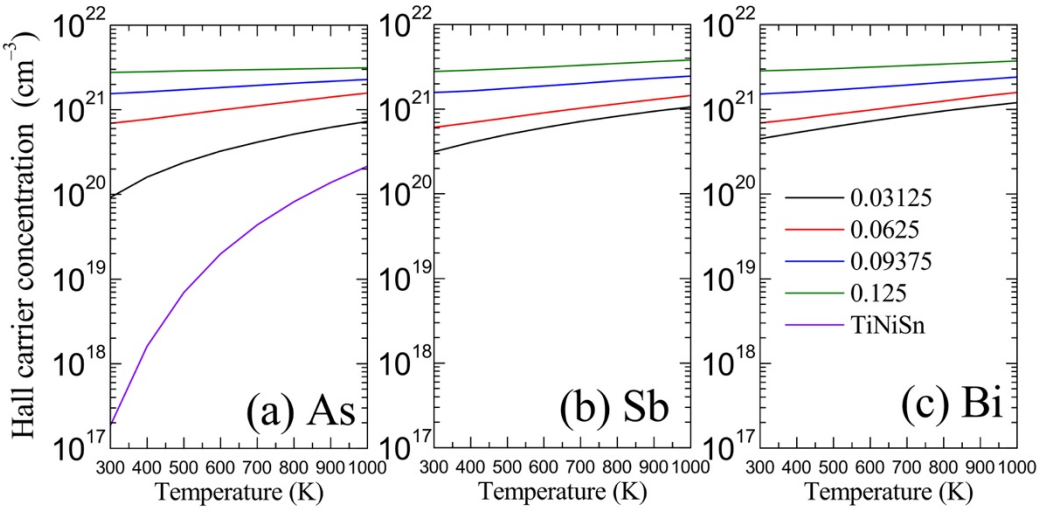

Figure 49 The Hall carrier concentration versus temperature for $TiNiSn_{1-x}A_x$ (A = As, Sb, and Bi; x = 0 – 0.125).

Summary

We successfully investigated the electronic and thermoelectric properties of $TiNiSn_{1-x}A_x$ (A = As, Sb, and Bi; x = 0 – 0.125). The electronic structure revealed the electron–filled state or electron pocket in the conduction band, it is an electron doping TiNiSn. The electrical conductivity and Hall carrier concentration increased with doping by As, Sb, and Bi. However, the power factor provided the maximum value in x = 0.03125 and 0.0625. In thermal part, the As, Sb, and Bi reduced the thermal conductivity by ~40%. The optimized ZT appeared in low doping concentration (x < 0.0625). The maximum ZT is 0.600 for $TiNiSn_{0.96875}As_{0.03125}$, 0.510 for $TiNiSn_{0.9375}Sb_{0.0625}$, and 0.515 for $TiNiSn_{0.96875}Bi_{0.03125}$, at 1000 K, respectively.